



Synthesis and application of stabilized zero-valent iron nanoparticles for hexavalent chromium removal in saturated sand columns: experimental and modeling studies

Amirhosein Ramazanpour Esfahani, Ahmad Farrokhian Firouzi*

Faculty of Agriculture, Department of Soil Science, Shahid Chamran University, Ahvaz, Iran, email: ramazanpour67@gmail.com (A. Ramazanpour Esfahani), Tel. +98 611 3742009; Fax: +98 611 3738282; emails: ahmad.farrokhian.scu@gmail.com, a.farrokhian@scu.ac.ir (A. Farrokhian Firouzi)

Received 8 January 2015; Accepted 8 July 2015

ABSTRACT

In the present study, simulation of hexavalent chromium (Cr(VI)) removal from saturated porous media using stabilized zero-valent iron nanoparticles (ZVIN) was carried out under different experimental conditions such as ZVIN concentration, initial Cr(VI) concentration, geochemistry of groundwater, and pore water velocity. In this regards, stabilized ZVIN was synthesized with two different stabilizers namely sepiolite and polyacrylic acid (PAA). The aims of this study were twofold: (1) a comparison between the efficiency of mineral-stabilized and polymer-stabilized ZVINs in Cr(VI) removal and (2) the simulation of the experimental data of Cr(VI) removal in a simulated groundwater system. The experimental data were interpreted using the convection–dispersion equation via the CXTFIT software. The colloidal stability of sepiolite-stabilized zero-valent iron nanoparticles (S-ZVIN) compared to PAA-stabilized zero-valent iron nanoparticles (PAA-ZVIN) was apparently high. Additionally, the results of reductive transport experiments showed that Cr(VI) removal had a direct relationship with ZVIN and chloride ion (Cl^-) concentrations, while an indirect relationship was observed with removal efficiency of Cr(VI) by initial Cr(VI) concentration and pore water velocity. Obtained simulated parameters (i.e. mass destruction term (μ) and retardation factor (R)) also confirmed the experimental results. Findings of both experimental and simulation studies indicated that clay mineral was absolutely more suitable than polymers as a stabilizer of ZVIN for reactive site treatment.

Keywords: CXTFIT; Groundwater; Hexavalent chromium; Polyacrylic acid; Sepiolite; Zero-valent iron nanoparticles

1. Introduction

Hexavalent chromium (Cr(VI)) is a poisonous metal that triggers a large number of human diseases such as ulcer, bronchitis, and liver damages [1].

Hazardous Cr(VI) principally originates from the discharges of tanning, textile, and paint manufacturing industries[2]. According to the United States Environmental Protection Agency (UEPA), 0.05 mg/L is set as a permissible limit of Cr(VI) in drinking water [3]. Therefore, excessive Cr(VI) concentrations in

*Corresponding author.

groundwater—as a source of potable water—should totally be removed.

In order to decrease Cr(VI) concentration to the permitted level, an innovative and environmentally friendly agent should undoubtedly be operated. In the last decade, zero-valent iron as a reductant and efficient agent has been used in permeable reactive barrier (PRB) systems to decrease the concentration of environmental pollutants under toxicity limit [4–6]. However, due, in part, to some economic and operational troubles, zero-valent iron nanoparticles (ZVIN) with high surface area and lower size that give them great capability to react with contaminants were replaced with previous technique. In a corresponding approach called the *in situ* technique, ZVIN with high concentrations was injected downward to contact with the contaminants in the aquifer or reach the target contaminants in the groundwater [7,8]. The versatility and the economic benefits of the *in situ* technique have provoked enthusiasm among the relevant engineers to focus on the technique and think about its application in contaminated sites.

Although the *in situ* approach was potentially a promising method, several challenges like aggregation, agglomeration, and the deposition of applied uncoated ZVIN have contributed to reduce its efficiency. Agglomerated ZVIN in the *in situ* technique dropped its reactivity with contaminants and caused pore clogging as well as a considerable decrease in the porosity of aquifers. Hence, in order to enhance *in situ* injection and delivery, ZVIN should be mobile and dispersed in aquifers.

To prevent ZVIN aggregation and attachment to the sand grains, surface modification of nanoparticles, among all proposed methods, is definitely an advantageous approach that creates electrostatic repulsive and steric forces which act against interparticle attraction forces and its attachment to porous media. Till now, there have been lots of polyelectrolytes (e.g. carboxymethyl cellulose (CMC) [9], polyacrylic acid (PAA) [10], polyvinylpyrrolidone [11,12], green polymers (e.g. guar gum [13,14] and starch [15]), and surfactants (e.g. sodium dodecylbenzenesulfonate (SDBS) [16]), which have generally been employed as stabilizers showing reasonable performances. Jiemvarangkul et al., as a brilliant example, demonstrated that PAA significantly enhanced the transport of ZVIN through a sand-packed column-like tracer [17]. Although the above-mentioned stabilizers provided significant colloidal stability and increased ZVIN transport in the subsurface environment, the drawbacks of their application such as the high cost of preparation and the environmental problems forced the researchers to devise an alternative.

Clays are intrinsically natural minerals that are widely applied as adsorbents for the removal of contaminants due, primarily, to their exclusive features such as high surface area and uptake capability [18]. Several researchers, in general, used different clay minerals for stabilizing ZVIN in order to enhance their reaction efficiency with pollutants [19,20]. For instance, Chen et al. demonstrated that Bentonite could play a key role in improving the colloidal stability of ZVIN that increased Methyl Orange (MO) removal from aqueous solution [21]. Sepiolite, among all clay minerals, as a porous and layered mineral with a large surface area, is considerably abundant in the central parts of Iran. Regarding such brilliant characteristics and the low cost, sepiolite-stabilized ZVIN (S-ZVIN) was synthesized as a novel and efficient nanocomposite in this study. To the best of our knowledge, no research has been carried out to compare the performance of polymer-stabilized and mineral-stabilized ZVIN for Cr(VI) removal in reactive zone systems. Consequently, it seems that any research aimed at clarifying the influence of mineral stabilizers compared to polymer stabilizers on the efficiency of ZVIN in the removal of contaminants from aquifers is a critical necessity, distinguishing it from the previous research. Therefore, sepiolite and PAA-stabilized ZVINs were synthesized to remove Cr(VI) from a simulated contaminated aquifer in sand-packed columns.

Until now, the majority of Cr(VI) removal studies using ZVIN has been performed in batch systems, [22–24] while a limited number of research has reported the results of their experiments in sand-packed columns [25,26]. Furthermore, categorized information about the quantitative investigations of contaminant removal in continuum systems are in rudimentary steps, although several qualitative contaminant treatments using ZVIN have been reported [27]. The simulation study of contaminant removal is a promising method to manage and determine the most proper adsorbent for environmental clean-up in reactive sites. That is why this study has focused on the simulation of Cr(VI) transport in sand-packed columns affected by two-stabilized ZVINs.

The aims of this research were: (1) the synthesis of stabilized ZVIN with PAA and sepiolite and their characterization, (2) the reductive removal of Cr(VI) using two-stabilized ZVINs in a sand-packed column under different experimental conditions such as ZVIN concentration, initial Cr(VI) concentration, groundwater chemical composition and pore water velocity, (3) the simulation of the experimental data of Cr(VI) removal in a simulated groundwater system, and (4) qualitative and quantitative comparisons between the

removal efficiency of Cr(VI) using two-stabilized ZVINS in order to find an appropriate stabilizer.

2. Experimental

2.1. Chemicals

In the present study, ferrous sulfate heptahydrate ($\text{FeSO}_4 \cdot 7\text{H}_2\text{O}$) was prepared from AppliChem Co., while PAA (750 K) was obtained from Sigma Aldrich Co. Moreover, sodium borohydride (NaBH_4), potassium dichromate ($\text{K}_2\text{Cr}_2\text{O}_7$), acetone, sodium hydroxide (NaOH), concentrated hydrochloric acid (12 N HCl), sodium chloride (NaCl), sodium dithionate, hydrogen peroxide, and 1,5 diphenylcarbazine were purchased from Merck Co. To prepare chromium solution, a specific amount of potassium dichromate was poured in a particular fraction of distilled water and kept at 4°C. Furthermore, the Iranian sepiolite was obtained from DaneshbonyanFarapouyanIsatis Co. Afterward, it was grounded using ball mill and then sieved by a 0.053 micrometer steel to reach the desirable size.

2.2. Synthesis of ZVINS

The PAA and sepiolite-stabilized ZVINS were prepared from the basis of the reduction of ferrous sulfate using borohydride in the presence of selected stabilizers as reported in the previous works [10,24]. PAA-ZVIN was synthesized through the addition of 20 mL of 1.05 M sodium borohydride solution (1.05 M NaBH_4) into 200 mL mixture of 100 mL of 0.065 M ferrous sulfate solution (0.065 M FeSO_4) and 100 mL of 0.05% w/v PAA solution using a dropping funnel in nitrogen gas atmosphere. During the injection of sodium borohydride in a 3 mL/min rate, the solution was stirred via a magnetic stirrer in high speed. After black particles appeared, it was stirred for an additional 30 min to control the diameter of ZVIN particles. The preparation of sepiolite-stabilized ZVIN was similar to PAA-ZVIN except using sepiolite instead of PAA as a stabilizer. Upon finishing the Fe and borohydride interaction, the supernatant was gathered using a strong magnet and washed with acetone and ethanol to remove the disturbing and undesirable ions.

The size, morphology, and surfaces of both synthesized ZVINS and raw sepiolite were determined using scanning electron microscope (SEM) (SEM, S 4160, Hitachi, Japan) and transmission electron microscope (TEM) (LEO-906E). The element composition on the structure of ZVINS and raw sepiolite was investigated using energy dispersive X-ray spectroscopy (EDS).

Finally, the hydrodynamic diameter and the zeta potential of ZVINS were measured via dynamic light scattering (DLS) instrument (DLS, Zetasizer, Malvern, UK) at a similar concentration and pH of 7. The colloidal stability of each synthesized ZVINS was performed to assess their resistance against deposition in aqueous media. Hence, 0.1 g/L of each ZVIN suspensions (with pH of 7) was prepared in the cell of UV-vis spectrophotometer and the absorbance of suspension was recorded at 508 nm wavelength in a quiescent condition during 120 min time period.

2.3. Porous media preparation

To carry out the Cr(VI) reductive transport study, sand grains were employed as the porous matrix. In this regard, sand particles with 2.68 g/cm³ specific gravity were sieved using a stainless steel 30–50 US mesh and reached the range of 300–600 µm. The process of preparation of sand particles was discussed in literature [28]. Briefly, in the first step, particles were immersed in 0.1 M sodium dithionate solution for approximately, 2 h to totally remove all the adsorbed metal oxides' impurities. Second, hydrogen peroxide solution (0.5% H_2O_2) was applied to remove organic matter for soaking the particles for 3 h. Eventually, these sand particles were soaked in 12 M hydrochloric acid (12 M HCl) overnight and washed with distilled water to keep constant pH of water and particles at 7.

2.4. Transport experiments

Reductive removal of Cr(VI) was carried out in saturated sand-packed columns under a steady state flow rate. To wet-pack the columns, small fractions of sand particles were poured sequentially into a 25-cm-long column with an inner diameter of 2.5 cm using a spatula until the column was filled. During the process of pouring the sand particles, in particular, the column was tapped with a plastic rod and gently vibrated to release any trapped air and get packed well. Furthermore, on the two sides of sand columns, a permeable screen diffuser was set to keep sand particles into the column. Prior to experiments, over 20 PVs of Cr(VI) solution with a typical concentration and pH of 7 were injected downward using a peristaltic pump connected to the inlet of sand column with a constant slow flow rate (0.05 cm/min) into the sand column to create a uniform Cr(VI) concentration and a steady state flow. The flow velocity of transport experiments was measured by weighing the collected water from the sand column into the samplers during specific time periods. A three-neck flask was used to keep the ZVIN suspension that

was equipped with N₂ gas to prevent ZVIN oxidation. Keeping ZVIN suspension in an isolated oxygen free chamber, in order to avoid oxidation has always been considered as a crucial agent in the field scale operation [29]. Furthermore, during ZVIN injection, the flask was put into the ultrasonic bath to homogenize the ZVIN suspension and decrease the aggregation of nanoparticles. Another peristaltic pump was set to inject downward the ZVIN suspension into the sand column during the injection of Cr(VI) solution with similar flow rate. The reductive transport survey of Cr(VI) was carried out with regards to different experimental variables including ZVIN concentration (2, 3, and 4 g/L), initial Cr(VI) concentration (40, 60, and 80 mg/L), chloride concentration (1, 10, and 100 mM), and pore water velocity (0.07, 0.1, and 0.15 cm/min). The schematic diagram of the experimental setup and the applied instruments has been illustrated in Fig. 1. During the experiments, each sample was gathered from the bottom of the sand column into the plastic bottles at different time intervals and then the residual Cr(VI) concentration was determined using diphenylcarbazide colorimetric method via a UV–visible spectrophotometer at a wavelength of 540 nm [30]. Table 1 illustrates the basic characteristics of the transport experiments.

2.5. Equation

The transport and reductive immobilization of Cr(VI) in saturated sand-packed columns as affected by ZVINS were simulated using convection-dispersion

Table 1
Characteristics of sand column

Item	Value
Column length (cm)	25
Column inner diameter (cm)	2.5
pH of solution	7
Porosity	0.36–0.39
ρ_b of sand column	1.62–1.68
Sand grain diameter (mm)	0.42
Temperature (K)	298

equation (CDE) [31]. The following one-dimensional equation (Eq. (1)) expressed the removal of Cr(VI) with a first-order mass-destruction term as follows:

$$R \frac{dC}{dt} = D \frac{d^2C}{dx^2} - v \frac{dC}{dt} - \mu C \quad (1)$$

where C is the Cr(VI) concentration (mg/L), x is the distance of Cr(VI) stream pathway (cm), t is the time (min), D is the longitudinal-dispersion coefficient (cm²/min), v is the flow velocity (cm/min), R is the retardation factor of Cr(VI) transport, and μ is the mass-destruction term (1/min). In the above-mentioned equation, two terms (i.e. R and μ) should be strictly considered to be able to describe the influence of both ZVINS on Cr(VI) transport and reduction. The high amounts of R and μ , in essence, implied more interaction between Cr(VI) and ZVIN, which led to

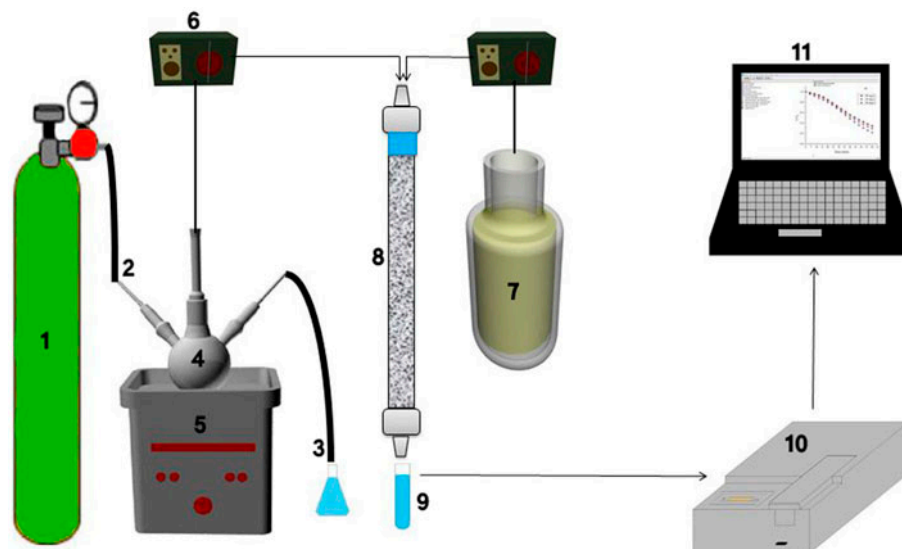


Fig. 1. Schematic illustration of experimental set up.

Notes: (1) Nitrogen chamber, (2) Nitrogen inlet, (3) Nitrogen outlet, (4) Three-neck flask, (5) Ultrasonic bath, (6) Peristaltic pump, (7) Chromium solution, (8) Sand column, (9) Effluent collector, (10) UV–visible spectrophotometer, and (11) Data logger.

decreasing the Cr(VI) concentration and retardation in Cr(VI) stream. The parameters D and v were calculated using nonlinear parameter optimization via Marquardt–Levenberg algorithm [32].

The transport curves of Cr(VI) were depicted based on the performed experiments and were also analyzed using CXTFIT software to fit the model parameters (R and μ). Using the following parameters, a quantitative comparison between the two applied ZVINS was carried out.

3. Results and discussion

3.1. Characterization

Fig. 2(a) shows the TEM image of needle-like sepiolite with their average sizes being around 1.6 μm . The SEM images of S-ZVIN and PAA-ZVIN are shown in Fig. 2(b) and (c). According to Fig. 2(b), sepiolite was bonded into the ZVIN particles and prevented particle aggregation. Furthermore, PAA-ZVIN was completely spherical and the sizes of both ZVINS were less than 100 nm (Fig. 2(c)).

To give further proof for interaction between sepiolite and ZVIN, EDS graphs of raw sepiolite, S-ZVIN, and PAA-ZVIN were prepared. Based on Fig. 2(d), four peaks (Si, Mg, Ca, and Al) were observed that indicated the presence of sepiolite. Moreover, in Fig. 2(e), an additional Fe peak together with the aforementioned sharp peaks was observed that could be assumed as an undeniable proof for bonding between ZVIN and sepiolite. Additionally, in the PAA-ZVIN EDS graph (Fig. 2(f)), sharp Fe and O peaks were obvious, which referred to ZVIN accompanied with Na and S ones derived from sodium borohydride and ferrous sulfate.

The colloidal stability of each applied nanoparticle was measured using a quantitative comparison of ZVIN deposition in a time period of 120 min. The cuvette containing 0.1 g/L of each ZVIN suspension with pH of 7 kept in fixed conditions with their absorbance recorded, using a spectrophotometer with a wavelength of 508 nm. According to Fig. 3, the majority of S-ZVIN particles (over 90%) was completely suspended during 120 min, while PAA-ZVIN showed lower suspended particles compared to S-ZVIN. This observation confirmed that in aqueous media, S-ZVIN had higher colloidal stability with higher discrepancy than PAA-ZVIN enabling it more able to transport and remove environmental contaminants. Besides, hydrodynamic diameter of 0.1 g/L of both ZVIN suspensions revealed that S-ZVIN (115 nm) had a smaller diameter than PAA-ZVIN (194 nm), which led to more

stability of S-ZVIN than PAA-ZVIN due to its lower deposition. The zeta potentials of S-ZVIN (−38.2 mV) and PAA-ZVIN (−29.1 mV) showed a complete coating of negative charges onto ZVIN surfaces created by stabilizers. Additionally, lower value of zeta potential of S-ZVIN compared to PAA-ZVIN proved higher colloidal stability of S-ZVIN than PAA-ZVIN.

3.2. Effect of ZVIN dosage

The concentration of applied ZVINS has significant impacts on the removal efficiency of Cr(VI). In a series of similar experiments, various ZVIN concentrations (2, 3, and 4 g/L) common in typical reactive sites were used to simulate the injection of ZVIN suspension into a polluted aquifer [33]. Other experimental variables including initial Cr(VI) concentration and pore water velocity were 50 mg/L and 0.05 cm/min, respectively. Fig. 4(a) and (b) shows that increasing the concentration of both ZVINS, caused a considerable enhancement in Cr(VI) removal efficiency. This may be related to increasing the number of reactive sites, creating a large capacity for Cr(VI) removal that logically abounds in higher ZVIN concentrations. So, Cr(VI) removal is a strongly concentration-dependent process. Although, the collision between particles is high in higher initial particle concentrations, the negative charges—that were created by stabilizers—onto the surfaces of ZVIN decreased their aggregation significantly. Therefore, high Cr(VI) removal was observed in higher initial ZVIN concentrations. The graphs for reductive transport of Cr(VI) as a function of ZVIN concentration were depicted based on the fraction of residual Cr(VI) (C) to initial Cr(VI) concentration (C_0) vs. reaction time (min) (Fig. 4(a) and (b)). For S-ZVIN, the maximum removal efficiency was 79.33% while, in similar ZVIN concentration, approximately maximum 66.04% of initial concentration of Cr(VI) was removed by means of PAA-ZVIN. The results of the simulation study of Cr(VI) removal are illustrated in Table 2. Looking closely, it is obvious that high coefficients of determination (R^2) (i.e. more than 0.95) approved the reliability of obtained parameters using the CXTFIT model. The quantitative study of Cr(VI) removal using S-ZVIN revealed that increasing S-ZVIN concentration, increased the mass-destruction term and the retardation factor from 0.00604 to 0.0548 and 1.12 to 1.98, respectively. For PAA-ZVIN, the above-mentioned parameters showed an increasing trend from 0.00105 to 0.00277 and 1.04 to 1.19, respectively. From the obtained results, it can be postulated that S-ZVIN compared to PAA-ZVIN is potentially more capable of

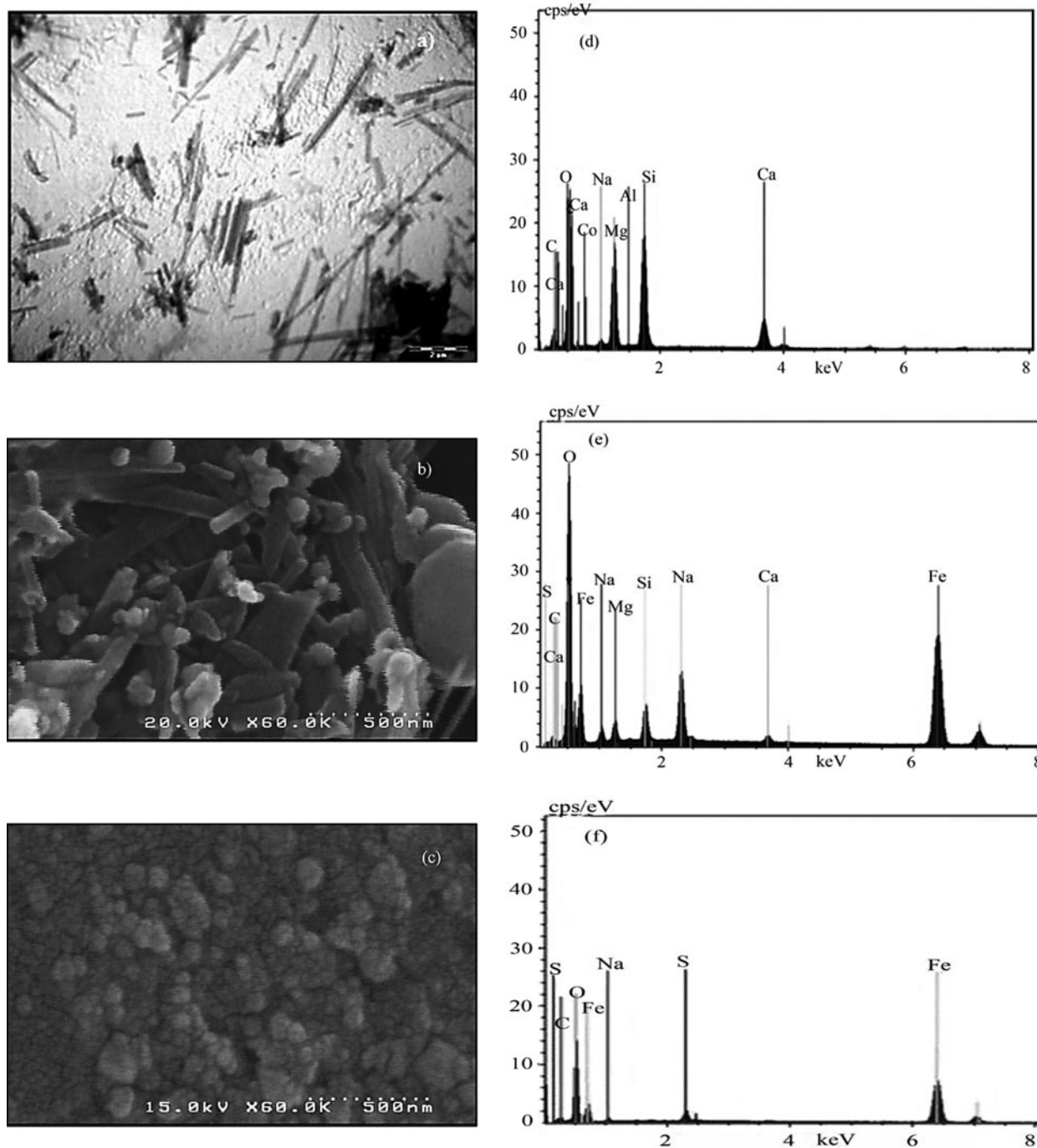
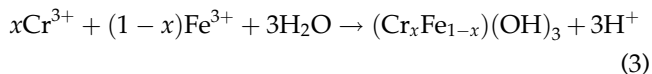
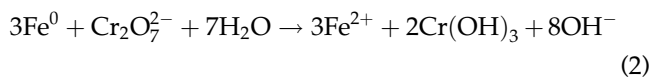


Fig. 2. (a) TEM image of sepiolite, (b) SEM images of S-ZVIN, and (c) PAA-ZVIN, (d) EDS diagrams of sepiolite, (e) S-ZVIN, and (f) PAA-ZVIN.

removing Cr(VI) from sand-packed columns. It has been proposed that the removal of Cr(VI) using ZVIN took place via joint reactions of reduction, precipitation, and co-precipitation of Cr(VI) according to the following equations [34]:



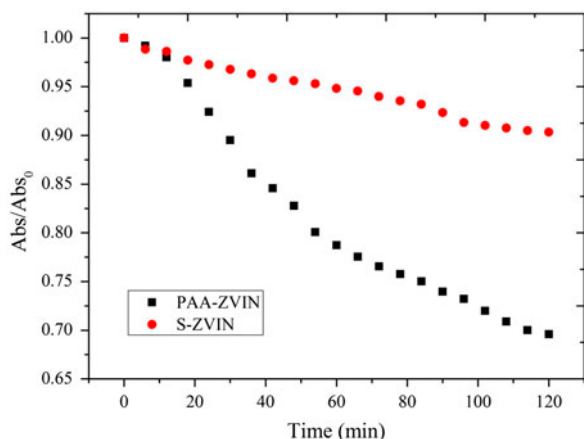


Fig. 3. Colloidal stability of the synthesized ZVINs (ZVIN concentration: 0.1 g/L and pH of solution: 7).

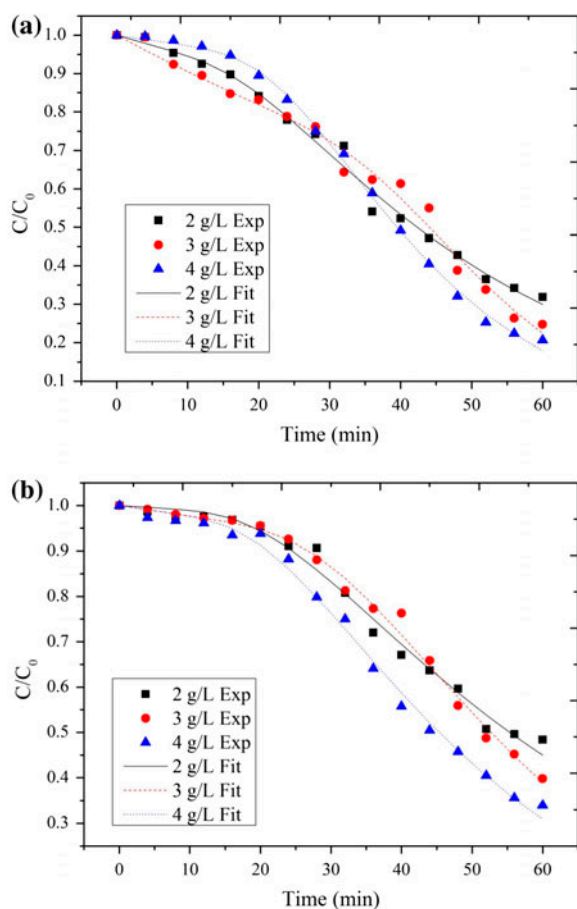
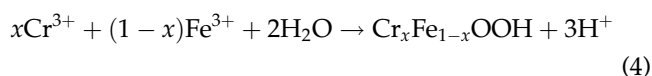


Fig. 4. Measured (symbols) and simulated (lines) data of Cr(VI) removal using (a) S-ZVIN and (b) PAA-ZVIN under 2, 3, and 4 g/L ZVIN concentrations (initial Cr(VI) concentration: 50 mg/L and pore water velocity: 0.05 cm/min).



The mechanism of Cr(VI) removal in sandy aquifer using ZVIN has been illustrated in Fig. 5. Based on Fig. 5, most of Cr(VI) concentration was reduced to trivalent chromium (Cr(III)), while minority of them was precipitated to $\text{Cr}_x\text{Fe}_{1-x}\text{OOH}$ and $\text{Cr}_x\text{Fe}_{1-x}(\text{OH})_3$ compounds.

3.3. Effect of initial Cr(VI) concentration

More experiments were performed to understand the effect of initial Cr(VI) concentration (40, 60, and 80 mg/L) in a saturated sand column on Cr(VI) removal efficiency using ZVINs. In these experiments, ZVIN concentration (2 g/L) and pore water velocity (0.05 cm/min) were kept constant. Initial Cr(VI) concentration, it was observed that it had a remarkable effect on Cr(VI) reductive removal with ZVIN. Results of the experiments revealed lower removal efficiency (in both ZVINs) when the initial Cr(VI) concentration rose. Fig. 6(a) shows that increasing the initial concentration of Cr(VI) from 40 to 80 mg/L, reduced sharply the removal efficiency from 74.74 to 65.38%. For PAA-ZVIN (Fig. 6(b)), in the same experimental conditions, and at the initial Cr(VI) concentration of 40, 60, and 80 mg/L the removal efficiency indexes were 55.23, 50.36, and 44.67%, respectively. As discussed above, it can be postulated that increasing Cr(VI) concentration creates a passivated Cr(VI) thin layer onto the outer surfaces of ZVIN, considerably limiting the electron transfer from Fe core to Cr(VI) and consequently, decreasing their reduction rate. In other words, the removal efficiency of Cr(VI) generally depends on the initial Cr(VI) concentration. According to Qiu et al., enhancing the initial Cr(VI) concentration from 5 to 20 mg/L caused a significant decrease in Cr(VI) removal efficiency using CMC-stabilized ZVIN [26]. The fitted parameters of Cr(VI) flow removal are also presented in Table 2. According to Table 2, it is clear that in different Cr(VI) concentrations of 40, 60, and 80 mg/L, the mass-destruction term were 0.012, 0.00745, and 0.00447 and the retardation factors were 1.15, 1.10, and 0.969, respectively. In the case of PAA-ZVIN, similarly, such simulated parameters (μ and R) were 0.000324, 0.00001, and 0.00001; and 0.770, 0.605, and 0.568, respectively. In consequence, from both the experimental findings and the simulated parameters, it is so tangible that S-ZVIN is apparently more capable of removing Cr(VI) from polluted-groundwater than PAA-ZVIN.

Table 2
Simulated parameters of Cr(VI) reductive transport using ZVINS in contaminated groundwater

ZVIN concentration (g/L)	Initial Cr(VI) concentration (mg/L)	Chloride concentration (mM)	Pore water velocity (cm/min)	S-ZVIN			PAA-ZVIN		
				μ	R	R^2	μ	R	R^2
2	40	0	0.05	1.20E-02	1.15E+00	0.982	3.24E-04	7.70E-01	0.9927
2	60	0	0.05	7.45E-03	1.10E+00	0.9886	1.00E-05	6.05E-01	0.9575
2	80	0	0.05	4.47E-03	9.69E-01	0.9878	1.00E-05	5.68E-01	0.9586
2	50	0	0.05	6.04E-03	1.12E+00	0.992	1.05E-03	1.04E+00	0.9882
3	50	0	0.05	1.42E-02	1.42E+00	0.993	2.71E-03	1.15E+00	0.9935
4	50	0	0.05	5.48E-02	1.98E+00	0.9981	2.77E-03	1.19E+00	0.9948
2	50	1	0.05	6.15E-03	2.76E+00	0.9621	2.94E-03	1.06E+00	0.9792
2	50	10	0.05	1.24E-02	2.97E+00	0.9919	4.23E-03	1.07E+00	0.9813
2	50	100	0.05	1.25E-01	3.79E+00	0.9928	4.92E-03	1.21E+00	0.9672
2	50	0	0.07	1.03E+00	5.20E-03	0.9804	9.53E-01	8.76E-04	0.9813
2	50	0	0.1	8.37E-01	3.06E-03	0.9755	8.34E-01	3.07E-04	0.9797
2	50	0	0.15	3.63E-01	1.43E-03	0.9659	2.42E-01	1.51E-04	0.9741

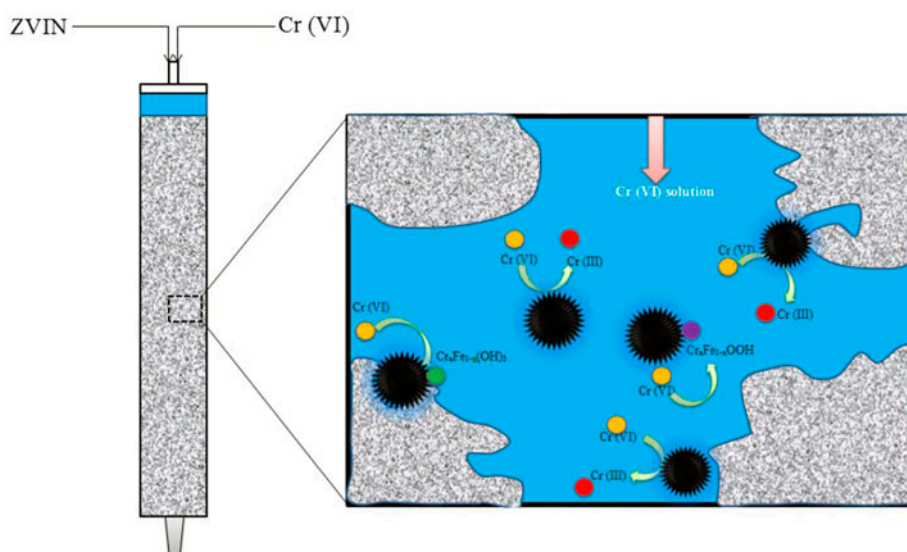


Fig. 5. Schematic mechanism of Cr(VI) removal in a flow system using ZVIN.

3.4. Effect of chloride concentration

Groundwater and aquifers contain either low or high amounts of anions that—perhaps produced as a result of the decomposition of minerals—have a significant role on the removal efficiency of contaminants using ZVIN. Among all typical anions, Cl^- is always considered as the most plentiful one. The experiments were carried out at different Cl^- concentrations in the range of 1–100 mM in order to evaluate the effect of ionic strength on Cr(VI) removal efficiency via ZVIN. The ZVIN concentration, the initial Cr(VI) concentration and the pore water velocity were considered as 2 g/L,

50 mg/L, and 0.05 cm/min, respectively. Based on Fig. 7(a) and (b), increasing Cl^- concentration from 1 to 100 mM has positive effects on Cr(VI) efficiency using ZVIN. Accordingly, the maximum Cr(VI) removal rate using S-ZVIN and PAA-ZVIN increased from 69.16 to 74.41% and from 52.48 to 58.02%, respectively. From Table 2, an enhancement is obvious in the quantity of mass-destruction term and retardation factor of Cr(VI) reductive removal using S-ZVIN and PAA-ZVIN. It is seen that for S-ZVIN, increasing Cl^- concentration from 1 to 100 mM caused a significant increase in μ and R from 0.00615 to 0.125 and 2.76 to 3.79, respectively. For

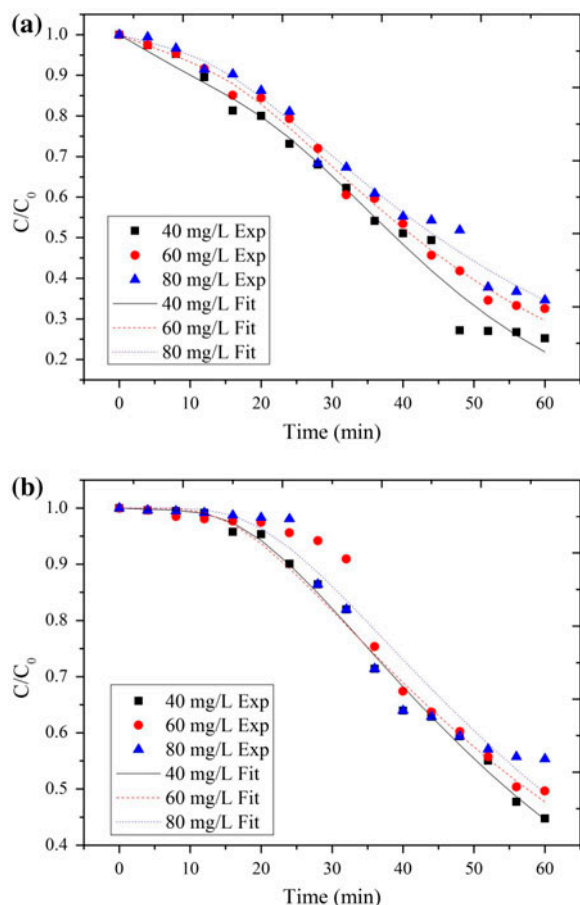


Fig. 6. Measured (symbols) and simulated (lines) data of Cr(VI) removal using (a) S-ZVIN and (b) PAA-ZVIN under 40, 60, and 80 mg/L Cr(VI) concentrations (ZVIN concentration: 2 g/L and pore water velocity: 0.05 cm/min).

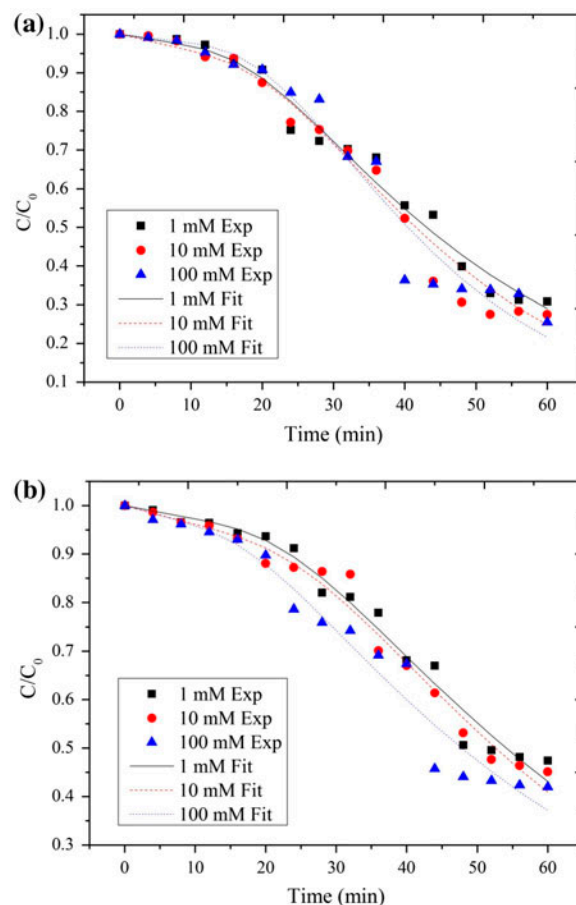


Fig. 7. Measured (symbols) and simulated (lines) data of Cr(VI) removal using (a) S-ZVIN and (b) PAA-ZVIN under 1, 10, and 100 mM chloride concentrations (ZVIN concentration: 2 g/L, initial Cr(VI) concentration: 50 mg/L and pore water velocity: 0.05 cm/min).

PAA-ZVIN, such parameters showed a similar trend where they rose from 0.00294 to 0.00492 and 1.06 to 1.21, respectively. Yin et al. reported that a huge improvement was observed in nitrobenzene removal in batch experiments as a result of increasing Cl^- concentration from 0 to 1,000 mg/L [35]. Chloride, it is believed, could destruct the hydroxide layer onto the surfaces of ZVIN and regenerate the reactive sites that gave capacity to ZVIN for Cr(VI) removal [36]. Unmistakably, high concentration of Cl^- is merely disadvantageous for the PRB technique for a long time. In the case of direct injection treatment, on the other hand, it is considered as an undeniable advantage, although it may cause retention and agglomeration of ZVIN.

3.5. Effect of pore water velocity

An additional factor that has a critical pattern on the Cr(VI) removal in each groundwater is pore water

velocity of flow in aquifers. In this research, the reductive transport of Cr(VI) using ZVIN was performed in various velocities (0.07, 0.1, and 0.15 cm/min) representing the range of the flow velocity of a typical groundwater. The other constant experimental variables were 2 g/L of ZVIN concentration and 50 mg/L initial Cr(VI) concentration. Fig. 8(a) and (b) illustrate the removal rate of Cr(VI) at different pore water velocities using S-ZVIN and PAA-ZVIN, respectively. Accordingly, Cr(VI) removal efficiency, in general, decreased considerably by increasing pore water velocity. Hosseini et al. also observed a sharp decrease in nitrate removal efficiency using Fe/Cu ZVIN by increasing pore water velocity from 0.0125 to 0.375 mm/s [27]. Going more into recorded data for S-ZVIN, maximum Cr(VI) removal rates were 67.46, 64.39, and 61.07% in 0.07, 0.1, and 0.15 cm/min pore water velocity, respectively. However, for PAA-ZVIN,

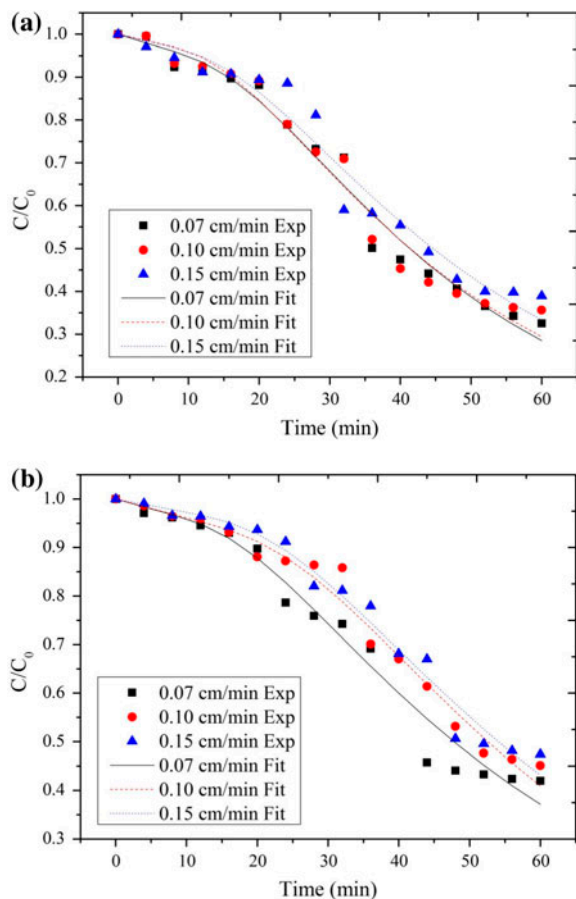


Fig. 8. Measured (symbols) and simulated (lines) data of Cr(VI) removal using (a) S-ZVIN and (b) PAA-ZVIN under 0.07, 0.1, and 0.15 cm/min pore water velocities: (ZVIN concentration: 2 g/L, initial Cr(VI) concentration: 50 mg/L).

over the same pore water velocity range, this rate dropped from 49.31 to 39.41%. The obtained simulated parameters for both ZVINs (Table 2) have a robust correlation with experimental results. It is clear that for S-ZVIN, from 0.07 to 0.15 cm/min pore water velocity, R and μ decreased from 0.0052 to 0.00143 and 1.03 to 0.36, respectively. A similar observation was reported for PAA-ZVIN, where in the same pore water velocity range, R and μ showed a decreasing trend from 0.0008757 to 0.000151 and 0.953 to 0.242, respectively. Higher flow velocity in each groundwater, in essence, reduces the reaction time and the interaction between ZVIN and the contaminants that leading to decrease in the removal efficiency.

4. Conclusion

In this study, the stabilized ZVINs with two different stabilizers including sepiolite and PAA were

synthesized and applied to eliminate Cr(VI) from saturated sand-packed columns. The influence of various experimental conditions such as ZVIN concentration, initial Cr(VI) concentration, geochemistry of groundwater, and pore water velocity of aquifer on the reduction of Cr(VI), breakthrough curves of Cr(VI) transport and parameters of CDE equation was investigated. Sepiolite, as an inexpensive and natural material, compared to PAA could certainly better protect the colloidal stability of ZVIN suspension and subsequently increased its interaction with Cr(VI). Reductive transport of Cr(VI) was assertively dependent on ZVIN concentration, initial Cr(VI) concentration, pore water velocity of contaminant flow, and the groundwater chemical compositions. Furthermore, the experimental curves of Cr(VI) reductive removal were perfectly fitted with the mathematical model based on CDE using CXTFIT. Results of the reductive flow experiments indicated that increasing ZVIN and chloride concentrations caused a significant improvement in the quantitative amount of mass-loss term and retardation factor. An increase in initial Cr(VI) concentration and pore water velocity, on the other hand, dropped the aforementioned simulated parameters. Ultimately, for the application of stabilized ZVIN in real reactive sites, mineral-stabilized ones, compared to polymer-stabilized ones, are highly recommended.

Acknowledgments

The authors would be so thankful to Shahid Chamran University of Ahvaz, Iran.

References

- [1] P. Kanmani, J. Aravind, D. Preston, Remediation of chromium contaminants using bacteria, *Int. J. Environ. Sci. Technol.* 9 (2012) 183–193.
- [2] M. Fabbicino, R. Gallo, Chromium removal from tannery wastewater using ground shrimp shells, *Desalin. Water Treat.* 23 (2010) 194–198.
- [3] D. Park, Y. Yun, J.M. Park, Studies on hexavalent chromium biosorption by chemically-treated biomass of *Ecklonia sp.*, *Chemosphere* 60 (2005) 1356–1364.
- [4] R. Baciocchi, M.R. Boni, L. D'Aprile, Characterization and performance of granular iron as reactive media for TCE degradation by permeable reactive barrier, *Water Air Soil Pollut.* 149 (2003) 211–226.
- [5] D.W. Blowes, C.J. Ptacek, S.G. Benner, C.W.T. McRae, T.A. Bennett, R.W. Puls, Treatment of inorganic contaminants using permeable reactive barriers, *J. Contam. Hydrol.* 45 (2000) 123–137.
- [6] T. Liu, I.M.C. Lo, Influences of humic acid on Cr(VI) removal by zero-valent iron from groundwater with various constituents: Implication for long-term PRB performance, *Water Air Soil Pollut.* 216 (2011) 473–483.

- [7] D.W. Elliott, W.X. Zhang, Field assessment of nanoscale bimetallic particles for groundwater treatment, *Environ. Sci. Technol.* 35 (2001) 4922–4926.
- [8] C.B. Wang, W.X. Zhang, Synthesizing nanoscale iron particles for rapid and complete dechlorination of TCE and PCBs, *Environ. Sci. Technol.* 31 (1997) 2154–2156.
- [9] Y.H. Lin, H.H. Tseng, M.Y. Wey, M.D. Lin, Characteristics of two types of stabilized nano zero-valent iron and transport in porous media, *Sci. Total Environ.* 408 (2010) 2260–2267.
- [10] A. Ramazanpour Esfahani, A. Farrokhian Firouzi, Gh. Sayyad, A. Kiasat, L. Alidokht, A.R. Khataee, Pb(II) removal from aqueous solution by polyacrylic acid stabilized zero-valent iron nanoparticles: Process optimization using response surface methodology, *Res. Chem. Intermed.* 40 (2014) 431–445.
- [11] A. Ramazanpour Esfahani, A. Farrokhian Firouzi, Gh. Sayyad, A. Kiasat, Transport and retention of two polymer-stabilized zero-valent iron nanoparticles in saturated porous media: Effects of initial particle concentration and ionic strength, *J. Ind. Eng. Chem.* 20 (2014) 2671–2679.
- [12] A. Ramazanpour Esfahani, A. Farrokhian Firouzi, Gh. Sayyad, A. Kiasat, Isotherm study of cadmium adsorption onto stabilized-zerovalent iron nanoparticles, *Int. J. Agron. Plant Prod.* 4 (2013) 3444–3454.
- [13] A. Tiraferri, K.L. Chen, R. Sethi, M. Elimelech, Reduced aggregation and sedimentation of zero-valent iron nanoparticles in the presence of guar gum, *J. Colloid. Interface Sci.* 324 (2008) 71–79.
- [14] A. Tiraferri, R. Sethi, Enhanced transport of zerovalent iron nanoparticles in saturated porous media by guar gum, *J. Nanopart. Res.* 11 (2009) 635–645.
- [15] F. He, D. Zhao, Preparation and characterization of a new class of starch-stabilized bimetallic nanoparticles for degradation of chlorinated hydrocarbons in water, *Environ. Sci. Technol.* 39 (2005) 3314–3320.
- [16] N. Saleh, H.J. Kim, T. Phenrat, J. Matyjaszewski, R.D. Tiltom, G.V. Lowry, Ionic strength and composition affect the mobility of surface modified Fe nanoparticles in water-saturated sand columns, *Environ. Sci. Technol.* 42 (2009) 3349–4455.
- [17] P. Jiemvarangkul, W.X. Zhang, H.L. Lien, Enhanced transport of polyelectrolyte stabilized nanoscale zero-valent iron (nZVI) in porous media, *Chem. Eng. J.* 170 (2011) 482–491.
- [18] G.J. Churchman, W.P. Gates, B.K.G. Theng, G. Yuan, Clays and clay minerals for pollution control, in: F. Bergaya, B.K.G. Theng and G. Lagaly (Eds.), *Handbook of Clay Science, Developments in Clay Science*, vol. 1, Elsevier, Oxford, UK, 2006, pp. 625–675.
- [19] X. Zhang, S. Lin, Z. Chen, M. Megharaj, R. Naidu, Kaolinite-supported nanoscale zero-valent iron for removal of Pb²⁺ from aqueous solution reactivity, characterization and mechanism, *Water. Res.* 45 (2011) 3481–3488.
- [20] Y. Zhang, Y. Li, J. Li, L. Hu, X. Zheng, Enhanced removal of nitrate by a novel composite nanoscale zero valent iron supported on pillared clay, *Chem. Eng. J.* 171 (2011) 521–531.
- [21] Z.X. Chen, X.Y. Jin, Z. Chen, M. Megharaj, R. Naidu, Removal of methyl orange from aqueous solution using bentonite-supported nanoscale zero-valent iron, *J. Colloid. Interface Sci.* 363 (2011) 601–607.
- [22] F. Fu, W. Han, C. Huang, B. Tang, M. Hu, Removal of Cr(VI) from wastewater by supported nanoscale zero-valent iron on granular activated carbon, *Desalin. Water Treat.* 51 (2013) 2680–2686.
- [23] B. Geng, Z. Jin, T. Li, X. Qi, Kinetics of hexavalent chromium removal from water by chitosan-Fe0 nanoparticles, *Chemosphere* 75 (2009) 825–830.
- [24] A. Ramazanpour Esfahani, S. Hojati, A. Azimi, L. Alidokht, M. Farzadian, A. Khataee, Reductive removal of hexavalent chromium from aqueous solution using sepiolite-stabilized zero-valent iron nanoparticles: Process optimization and kinetic study, *Korean. J. Chem. Eng.* 31 (2014) 630–638.
- [25] C. Mystrioti, A. Xenidis, N. Papassiopi, Reduction of hexavalent chromium with polyphenol-coated nano zero-valent iron: column studies, *Desalin. Water Treat.* (in-press), doi: 10.1080/19443994.2014.941298.
- [26] X. Qiu, Z. Fang, X. Yan, F. Gu, F. Jiang, Emergency remediation of simulated chromium(VI)-polluted river by nanoscale zero-valent iron: Laboratory study and numerical simulation, *Chem. Eng. J.* 193–194 (2012) 358–365.
- [27] S.M. Hosseini, B. Ataie-Ashtiani, M. Kholghi, Nitrate reduction by nano-Fe/Cu particles in packed column, *Desalination* 276 (2010) 214–221.
- [28] F. He, M. Zhang, T. Qian, D. Zhao, Transport of carboxymethyl cellulose stabilized iron nanoparticles in porous media: Column experiments and modeling, *J. Colloid. Interface Sci.* 334 (2009) 96–102.
- [29] C.C. Chien, H.I. Inyang, L.G. Everett, *Barrier Systems For Environmental Contaminant And Treatment*, CRC Press Taylor & Francis Group, Boca Raton, FL, 2006, p. 409.
- [30] V.K. Gupta, J. Suhas, Application of low-cost adsorbents for dye removal—A review, *J. Environ. Manage.* 90 (2009) 2313–2342.
- [31] J.C. Parker, M.T. Van Genuchten, Determining transport parameters from laboratory and field tracer experiments, *Bull.* 84–83. Virginia. Ag. Exp. Station, Blacksburg, VA, 1984.
- [32] D.W. Marquardt, An algorithm for least-squares estimation of nonlinear parameters, *J. Appl. Math.* 11 (1963) 431–441.
- [33] N. Saleh, Surface modifications enhance nanoiron transport and NAPL targeting in saturated porous media, *Environ. Eng. Sci.* 24 (2007) 45–57.
- [34] X.Q. Li, J.S. Cao, W.X. Zhang, Stoichiometry of Cr(VI) immobilization using nanoscale zerovalent Iron (nZVI): A study with high-resolution X-ray photoelectron spectroscopy (HR-XPS), *Ind. Eng. Chem. Res.* 47 (2008) 2131–2139.
- [35] W. Yin, J. Wu, P. Li, X. Wang, N. Zhu, P. Wu, B. Yang, Experimental study of zero-valent iron induced nitrobenzene reduction in groundwater: The effects of pH iron dosage oxygen and common dissolved anions, *Chem. Eng. J.* 184 (2012) 198–204.
- [36] L.J. Matheson, P.G. Tratnyek, Reductive dehalogenation of chlorinated methanes by iron metal, *Environ. Sci. Technol.* 28 (1994) 2045–2053.